



OPEN ACCESS

EDITED BY
Matjaž Perc,
University of Maribor, Slovenia

REVIEWED BY
Federico Musciotto,
Central European University, Hungary
Ginestra Bianconi,
Queen Mary University of London,
United Kingdom

*CORRESPONDENCE
Alessandro Vezzani,
alessandro.vezzani@unipr.it

SPECIALTY SECTION
This article was submitted to Social
Physics,
a section of the journal
Frontiers in Physics

RECEIVED 03 August 2022
ACCEPTED 26 September 2022
PUBLISHED 25 October 2022

CITATION
Guizzo A, Vezzani A, Barontini A,
Russo F, Valenti C, Mamei M and
Burioni R (2022), Simplicial temporal
networks from Wi-Fi data in a university
campus: The effects of restrictions on
epidemic spreading.
Front. Phys. 10:1010929.
doi: 10.3389/fphy.2022.1010929

COPYRIGHT
© 2022 Guizzo, Vezzani, Barontini,
Russo, Valenti, Mamei and Burioni. This
is an open-access article distributed
under the terms of the [Creative
Commons Attribution License \(CC BY\)](https://creativecommons.org/licenses/by/4.0/).
The use, distribution or reproduction in
other forums is permitted, provided the
original author(s) and the copyright
owner(s) are credited and that the
original publication in this journal is
cited, in accordance with accepted
academic practice. No use, distribution
or reproduction is permitted which does
not comply with these terms.

Simplicial temporal networks from Wi-Fi data in a university campus: The effects of restrictions on epidemic spreading

Andrea Guizzo^{1,2}, Alessandro Vezzani^{1,2,3*}, Andrea Barontini⁴,
Fabrizio Russo⁴, Cristiano Valenti⁴, Marco Mamei^{5,6} and
Raffaella Burioni^{1,2}

¹Dipartimento di Scienze Matematiche, Fisiche e Informatiche, Università degli Studi di Parma, Parma, Italy, ²INFN, Sezione di Milano Bicocca, Gruppo Collegato di Parma, Parma, Italy, ³Istituto dei Materiali per l'Elettronica ed il Magnetismo (IMEM-CNR), Parma, Italy, ⁴U.O. Sistemi Tecnologici e Infrastrutture, Area Sistemi Informativi, Università degli Studi di Parma, Parma, Italy, ⁵Dipartimento di Scienze e Metodi dell'Ingegneria, Università di Modena e Reggio Emilia, Reggio Emilia, Italy, ⁶Artificial Intelligence Research and Innovation Center—AIRI, Università di Modena e Reggio Emilia, Modena, Italy

Wireless networks are commonly used in public spaces, universities, and public institutions and provide accurate and easily accessible information to monitor the mobility and behavior of users. Following the application of containment measures during the recent pandemic, we analyzed extensive data from the Wi-Fi network in a university campus in Italy during three periods, corresponding to partial lockdown, partial opening, and almost complete opening. We measured the probability distributions of groups and link activations at Wi-Fi access points, investigating how different areas are used in the presence of restrictions. We ranked the hotspots and the area they cover according to their crowding and to the probability of link formation, which is the relevant variable in determining potential outbreaks. We considered a recently proposed epidemic model on simplicial temporal networks, and we used the measured distributions to infer the change in the reproduction number in the three phases. Our data show that additional measures are necessary to limit the spread of epidemic in the total opening phase due to the dramatic increase in the number of contacts.

KEYWORDS

epidemic spread, Wi-Fi datasets, simplex size distribution, temporal network, containment measures

1 Introduction

Wireless networks are increasingly used in public spaces as a tool to provide constant connectivity over large areas for diversified devices. Organized in widespread and economic hotspots, wireless networks, in contrast to mobile networks, are particularly accessible to researchers because their use is common in university and corporate campuses and, in general,

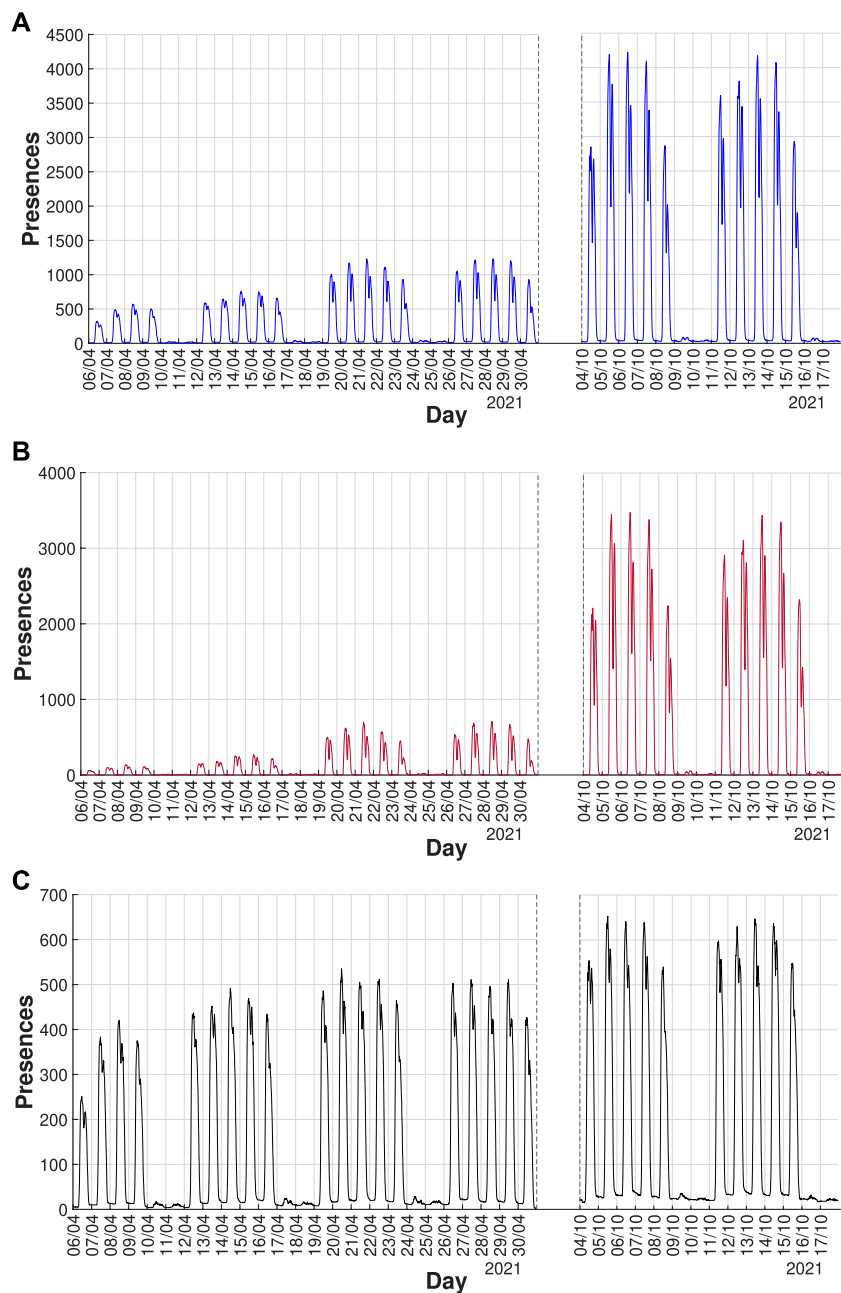


FIGURE 1

Dynamical behavior of attendance at Parma University. Plot of temporal evolution of the attendance of all users (A), students (B), and structured staff (C) during the different closing phases. The first 2 weeks correspond to the closing phase, the two central weeks to the partial opening phase, and the last 2 weeks to the total opening phase. We can observe a significant increase in attendance for students in different phases, while for structured staff, we find a very similar dynamical behavior of attendance between different regimes. The data are very detailed and give much information, such as the low number of attendances during the weekend and during holidays.

in institutions with interest in primary research. Data from wireless networks have often been analyzed to measure the quality of service and to improve network performance and management [1, 2]. However, they also provide accurate and easily accessible data, which allows us to study user mobility, physical space fruition, and user behavior [3, 4].

Monitoring the occupation of public spaces by many people at the same time has become particularly interesting in the last 2 years, during the COVID-19 pandemic. In fact, in this last period, it has become of fundamental importance to be able to control crowded areas to maintain adequate distancing measures. Large events and gatherings, in particular those taking place indoors, have been often

related to super-spreading events that have accelerated the outbreaks [5]. Therefore, they should be monitored. On the other hand, social distancing creates enormous economic and social costs. It is, thus, important to adequately control large gatherings in public spaces and, at the same time, quantify the benefits of different containment measures.

In this respect, Wi-Fi data represent an extremely interesting tool. They are easily available through public institutions, and they rely on relatively economic infrastructures that are already present in public spaces. The localization of agents is not as accurate as for GPS and mobile traces [6–8], but it can be improved with different tools. Interestingly, Wi-Fi data directly provide the distribution of clusters of users connected to the same access point, potentially crowding the same area and forming temporal simplices which evolve in time [9, 10]. This is relevant information to be used as an input for models of higher-order interactions in epidemics and information spreading with complex contagions [11–13].

Considering the problem of pandemic control, in this study, we explore Wi-Fi data from the university campus in Parma, Italy, to monitor both the formation of large gatherings and the presence of areas of intense traffic. We follow the daily usage of public areas across the campus from anonymized data of devices connected to the access points (APs) of the network. In particular, we measure the probability distribution of large gatherings and of the number of different couples (links) generated at the same spot, potentially accounting for dangerous contacts, in specific areas of the campus. We analyze three phases, characterized by different containment measures: a closing phase, a partial opening phase, and an open phase, with almost complete reopening of the university activities. Based on this analysis, we rank the APs according to their potential danger and we characterize the fruition of spaces by different classes of users in the three periods. In particular, we show that the attendance data in the closing phase follow a completely different distribution, while the two opening phases share similar features, after a proper rescaling of the total numbers of users. Relying on a recent modelling scheme of epidemic propagation in activity-driven simplicial temporal networks [9, 10, 14, 15], we also estimate the change in the reproduction rate R_0 due to the release of restrictions in the last period. Our data signal a dramatic change in the reproduction number, suggesting that additional measures are crucial to limit the probability of outbreaks in the open phase.

2 Wi-Fi data

2.1 Attendance data in the presence of different containment measures

The University of Parma, like many universities and public institutions, has covered its buildings and spaces with a unified

Wi-Fi network, enabling all users to establish more than 10,000 sessions a day. All session data from the login management system are collected by the “ICT services” office of the University of Parma. The login management system manages all wireless APs and all users’ requests for connection to the internet with their registered devices.

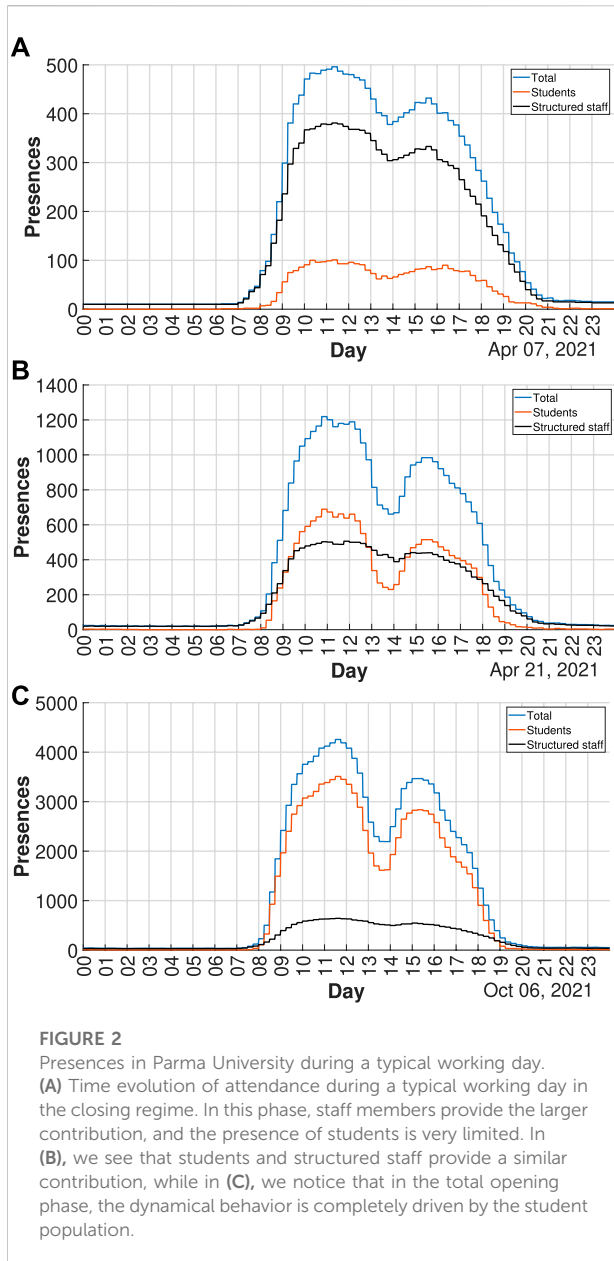
The staff of the “ICT service” office has the authorization to access files with personal data and carry out an anonymization process. The structure of the dataset and the anonymization process is described in the [Supplementary Appendix](#). From the anonymized data, we infer the number of individuals and the number of different couples per day in specific areas, avoiding double-counting of the same individual in a 24-h time window. These data do not any contain personal information.

The resulting dataset refers to a sample of 696 wireless APs, 19,749 users (divided into 16,505 students, 1,968 structured staff, and 1,276 external guests), and about 15,000 daily connections. The dataset spans 10 months, starting on December 10TH 2020 and ending on November 7TH 2021. During this period, due to the COVID-19 pandemic restrictions, we can distinguish three different phases: a closing phase, a partial opening phase, and a total opening phase for the 2021-2022 academic year.

- Closing phase. During this phase, access to university buildings was allowed only to staff, faculty, and students who took part in laboratory activities. All lectures were held remotely. This phase starts on December 10TH 2020 and ends on February 21TH 2021 and starts again on February 21TH 2021 and ends on April 18TH 2021.
- Partially opening phase. During this phase, access to the university buildings was extended to first-year students to allow them to follow lessons in limited presence (about 25% of students enrolled in the degree courses). This phase starts on February 22TH 2021, ends on March 14TH 2021 and starts again on April 19TH 2021, finally ending in June.
- Total opening phase. During this phase, teaching activities took place in classrooms with the request of a Green Pass to access the university. This phase starts on September 27TH 2021 and ends with our dataset.

2.2 Dynamical behavior of attendance data

From the connection session, we can estimate the time evolution of the attendance at a single AP, in a university building or area (such as the scientific campus) or in the whole university. To obtain these data, we extract from the connection sessions the number of users connected to each AP as a function of time, every minute. The sum of all AP’s



temporal series corresponds to the presences for the entire university or for the campus APs. The algorithm also extracts the dynamical behavior of attendance for generic users and, separately, student users, structured staff, and external guests. In Figure 1, we graphically represent attendance data at the university in the different phases of closures. For structured staff, we find a very limited increase in attendance in the second and third regimes, while the presence of students increases very significantly in the last phase.

Figure 2 shows the attendance data in the university on a typical working day during the closing Figure 2A, the partial

opening Figure 2B, and the total opening Figure 2C phases. In all cases, the curve rapidly increases in the morning, partially decreases during lunchtime, increases again in the afternoon, and decreases in the evening. We notice that in the closing phase, staff members provide the largest contribution, which is similar to the partial opening phase. On the other hand, in the total opening phase, the behavior is totally driven by the student population. Moreover, the student population displays an oscillating behavior, with peaks corresponding to the morning and afternoon lessons, while the presence of staff members is distributed during the whole working hours.

As mentioned above, Wi-Fi data only refer to individuals connected to the Wi-Fi, and this naturally leads to an underestimation of the total number of presences. To measure such an effect, we compared the Wi-Fi data with data obtained from the badge access to a specific building (the physics building). For this calibration, we restrict our measure to structured staff in the partial opening phase. Indeed, only in this case, the use of the badge was compulsory. Figure 3 shows that the attendance given by Wi-Fi data is underestimated about by a factor of 2 compared to the attendance given by badge data. To obtain an analogous calibration for the student dataset, we compared Wi-Fi data from APs near a specific classroom (“Aula Newton”) inside the physics building with the online seat reservation needed to take part in the face-to-face lessons during the partial opening phase. Also, in this case, we find an underestimation of the Wi-Fi data by about a factor of 2 compared to that of online seat reservations.

2.3 Data limitations

Passive Wi-Fi data at the AP level is a coarse measure for people localization and co-location. Depending on multiple factors like signal strength and load on individual APs, devices in different rooms can connect to the same AP, or *vice versa*, devices in the same room can connect to different APs [16]. A number of technologies exist to improve this kind of localization (see Section 2.4); however, they either require special sensing applications installed on the devices or special sensors on the APs. None of them is widely available and deployed. Instead, our goal is to investigate results coming from the Wi-Fi-infrastructure “AS-IS” deployed nowadays in the majority of buildings and public spaces.

Due to localization errors, some of the results described in the next section can contain miscounts (e.g., people connected to the AP registered in a room that was actually another one). However, the university buildings are large, with large classrooms and halls [17–19], and over long observation periods, these errors will likely average out, as it is more likely to be connected to the AP in the room where the device is actually present. Therefore, we

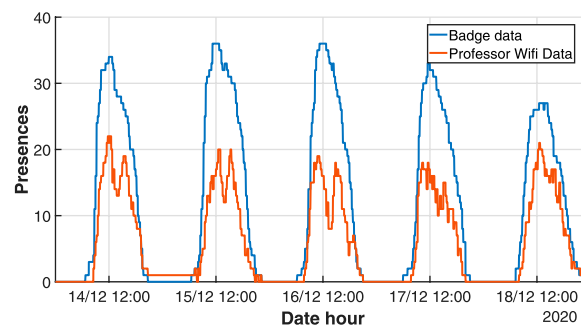


FIGURE 3

Wi-Fi data calibration. A comparison of the temporal evolution of attendance obtained from badge reader (blue line) data and from the Wi-Fi data for structured staff (red line) during a typical working week. The attendance obtained from Wi-Fi is underestimated by about a factor of 2 compared to the attendance provided by badge data.

believe such mis-locations are limited in our scenario. In this perspective, the comparison between Wi-Fi data and badge readings reported in Figure 3 confirms that our method provides reliable results.

Moreover, we stress that our results are typically based on the comparison between different time periods characterized by different opening and closing phases. Therefore, it is likely that possible errors are cancelled out since the number of miscounts due to limitations of our technologies should affect the different phases in the same manner. Accordingly, we are confident that our results and conclusions hold despite data limitations and that the advantages of using “standard” passive Wi-Fi data, both in terms of widespread applicability and in terms of allowing a long-term indefinite observation period, outweigh the limitations.

2.4 Monitoring crowding with different approaches

There are several ways to use Wi-Fi networks to localize and estimate people’s presence in an environment. We briefly summarize them and discuss applications of Wi-Fi localization, and also other technologies, to analyze COVID-related crowding.

2.4.1 Improved Wi-Fi-based measures for people counting

A number of technologies have been proposed to use the Wi-Fi network as a means to localize and estimate people’s presence. One of the key advantages of our proposal is to rely on the available Wi-Fi-infrastructure “AS-IS.” Even if the precision obtained in people localization is limited, the approach can be immediately applied to a wide range of

environments for a prolonged indefinite period of observation, providing sufficiently accurate measures of occupancy. Nevertheless, we think it is valuable to briefly survey existing approaches that could be used to improve Wi-Fi localization with special-purpose equipment that could be installed in critical areas.

Wi-Fi Real-Time Location System (RTLS) [4, 20, 21] uses multiple network signals (e.g., Received Signal Strength–RSS, Angle of Arrival–AoA) from multiple neighboring APs to provide high precise localization of individual devices. Reports indicate that the RTLS can achieve localization accuracy of less than 5–10 m.

An even more advanced technique, the analysis of WiFi Channel State Information can detect and count people’s presence (actual people, not devices) in an environment. In particular, [22] analyzed this technique (that requires specifically placed hardware) for COVID-Safe Occupancy Monitoring, obtaining optimal performance.

A number of studies, e.g. [3], use specific apps to track and localize individuals based on Wi-Fi signals. Continuous tracking *via* specific apps can notably improve localization accuracy, but it requires users to actively install the application. Also, approaches like the one in [16] would notably improve Wi-Fi localization accuracy but critically require Wi-Fi signal sensing by the smartphone—therefore reacquiring specific (monitoring) apps to be installed. Similarly [23], we apply advanced estimation mechanisms to calibrate Wi-Fi measures on the basis of camera footage. After a calibration phase, they achieve improved performance on people counting.

This kind of technology would notably improve our estimates, but it is not widespread in Wi-Fi deployments and does not need the involvement of multiple users; therefore, it cannot be directly applied without notable investments.

2.4.2 Systems for the analysis of distancing

There are also some available approaches to detect distancing in general, not Wi-Fi-based, which we briefly review here.

Mobile phone applications have been one of the most used technologies to monitor social distancing and track COVID diffusion [24, 25]. In this context, Bluetooth-inferred proximity [16, 26] is one of the most commonly used technologies. These approaches basically rely on mobile phones' localization and/or detection of nearby devices to detect social distancing. As well-documented in mainstream news, the main issue with this technology is user acceptance and willingness to actively install such applications.

Another important body of work is about monitoring large user populations *via* mobile phone networks [27]. A number of network signals are recorded by mobile phone operators and can be used to effectively localize individuals and analyze social distancing. While these applications can cover large areas, network-based localization accuracy is often too coarse to detect social distancing.

The recent advancements in computer vision technology and widespread deployment of fixed and mobile cameras (e.g., on drones) have attracted a number of works analyzing social distancing on the basis of video analysis [28]. From a technological point of view, this is probably one of the best solutions, but it is hindered by strong privacy concerns about accessing multiple video feeds.

More in general, [29] introduces several challenges in multiple technologies to contact tracing and analysis of social distances.

2.4.3 Wi-Fi-based systems for the analysis of distancing

Restricting our focus on Wi-Fi-based approaches to monitor distancing, we find different directions.

The work in [30] analyzes user occupancy and mobility *via* deployed Wi-Fi infrastructure to help institutions monitor and maintain safety compliance according to the public health guidelines. While the overall motivations and goals of this work are very similar to ours, there are some important differences with regard to the metrics derived from Wi-Fi data. In our analysis, we strived to be fully GDPR-compliant. Therefore, analysis/applications requiring maintaining user-ID for a prolonged time—like the mobility analysis conducted in this related work—are actually unfeasible under GDPR. *Vice versa*, we identified novel, useful, and GDPR-compliant analyses—e.g., the AP different links per day—that can better support institutions. Similarly, [31, 32], describes a similar analysis with the aforementioned differences with our approach.

Analogously [33], it presents a system to observe individuals and spaces to implement policies for social distancing and contact tracing using Wi-Fi connectivity data in a passive and privacy-preserving manner.

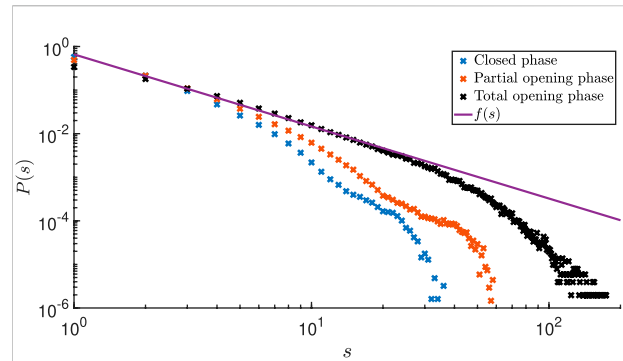


FIGURE 4

University group size distribution. Probability $P(s)$ to find a group of s people connected to the same AP for almost 15 consecutive minutes on a log–log scale. We plot the group size probability distribution for each phase with different restriction regimes. The distribution $P(s)$ in the total opening phase is compatible with a power law $f(s) \propto s^{-\gamma}$ with an exponent $\gamma \approx 1.65$.

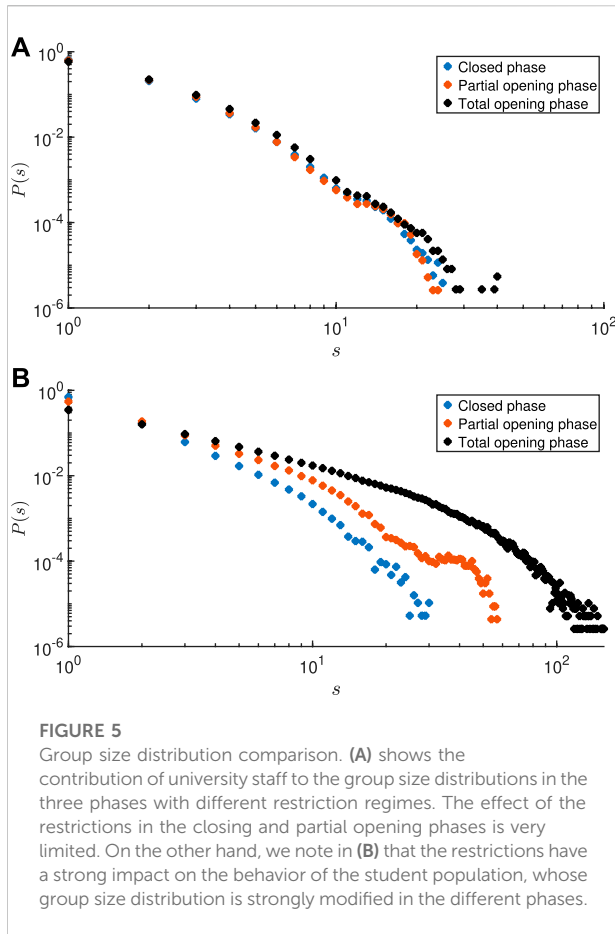
One of the most interesting related works is [34]. They start from motivations similar to ours and compute analogous co-location metrics. However, their approach does not take into consideration “forced” distancing in some environments and cannot differentiate between “safe” areas with numerous co-locations but distanced between each other (e.g., classes) and “unsafe” areas where distancing is not enforced (e.g., hallways). On the other hand, our work presents a compelling analysis of the localized closure policies that can be enacted on the basis of the obtained results. Such policies could be effectively implemented using our data and approach.

Similarly, the recent work [35] discusses passive Wi-Fi-monitoring in a campus scenario to monitor social distances. While their goals, motivations, and technologies being very similar to ours, our work focuses on a much longer monitoring period to analyze the impact of different policies enacted to contain COVID epidemics. Moreover, our work applies novel analysis to better-measure epidemiology.

3 Results

3.1 The simplex size distribution

During the COVID-19 pandemic, great attention has been devoted to limiting large gatherings of people, especially in situations where the tracing of the attendance is a difficult task. In this framework, the Wi-Fi dataset provides a natural way of monitoring the presence of large groups (simplices) within a certain area by considering the number of people simultaneously connected to the same AP. As a first step, we extract the group size s distribution $P(s)$ from Wi-Fi data connections during working hours (from 8.00 a.m. to 7.00 p.m.).



In social systems, the duration in time of face-to-face contacts typically displays a broad distribution with non-trivial behaviors [36, 37]. However, the infection process occurs on a characteristic timescale, which for COVID-19 has been estimated to be about 15 min for the first variants [38]. We, therefore, define a simplex of size s a group of s people who are connected to the same AP for at least 15 min (the same time interval used in contact tracing apps). Since this choice can influence the cluster size distribution, we also verify that our main results are qualitatively independent of this choice, by varying the time interval from 5 to 30 min. In particular, for each AP, we split working hours (from 8.00 a.m. to 7.00 p.m.) into 15-min intervals, and for each interval, we find the number of users that were connected to that AP for the entire time interval: this number corresponds to the simplex size. Disconnections from a single AP lasting less than 5 min have been discarded from our data set. We distinguish the three phases of the pandemic period with different levels of restriction (closing, partially opening, and total opening phases) and obtain three different distributions of group sizes.

Figure 4 clearly shows that a broader distribution $P(s)$ is observed in the opening phases, and the maximum group size grows from $s_{\max}^C = 36$, to $s_{\max}^{PO} = 58$ and to $s_{\max}^{TO} = 174$ in the

closing, partial opening, and opening phases, respectively. In particular, the distribution $P(s)$ in the total opening phase is compatible with a power law $P(s) \propto s^{-\nu}$ with an exponent $\nu \approx 1.65$. In Figure 5 we plot the different contributions of university staff and students to the group size distribution. Again, the plot clarifies that the restrictions in the closing and partial opening periods mainly affect the behavior of the student population, whose simplex distribution is strongly modified in the different phases, while for staff members, the differences are very limited.

3.2 Epidemics on simplicial temporal networks

Epidemic compartmental models have recently been extended to time-evolving networks driven by the activity of nodes in the framework of activity-driven networks [39–41]. In particular, in simplicial activity-driven networks [9, 10], nodes are grouped into fully connected clusters of different sizes, which are continuously activated and destroyed. In this context, parameters tailored to SARS-CoV-2 transmission [42–44] have been considered.

In the susceptible–infected–recovered (SIR) model on activity-driven simplicial networks [9, 10], the interaction network evolves by activating simplices at rate a , the simplex activity; when a simplex (clique) of size s is active, s nodes are chosen uniformly at random to participate in the simplex, producing $s(s-1)/2$ interactions. Then, the cluster is destroyed, and the process is iterated. The simplex size s is drawn from the distribution $P(s)$ of the sizes of the clusters, which models the heterogeneity in the size of gatherings. Each susceptible node of the cluster is infected with a probability λ by the infected nodes I that belong to the same cluster. Then, each node randomly recovers at a rate μ , as in the original SIR. The epidemic propagation is governed by the basic reproduction number R_0 : if $R_0 < 1$, the epidemic does not spread and only a finite number of people are infected, while for $R_0 > 1$, the epidemics display an exponentially growing outbreak, eventually infecting a finite fraction of the whole population. Since in the network evolution, each simplex is randomly reconstructed at each activation so that the connections among the agents are continuously reshuffled, a mean field approach exactly describes the evolution of the system:

$$\begin{aligned} \partial_t S(t) &= -S(t) \int asP(s) [1 - (1 - \lambda I(s))^{s-1}] ds \\ \partial_t I(t) &= -\mu I(t) + S(t) \int asP(s) [1 - (1 - \lambda I(s))^{s-1}] ds \\ \partial_t R(t) &= \mu I(t) \end{aligned} \quad (1)$$

where a is the activation rate of a simplex (i.e., the number of simplices in the system per unit of time), λ is the probability

that an active link transmits the disease, and μ is the recovery rate of a node. $S(t)$, $I(t)$, and $R(t)$ represent the probabilities for a node to be susceptible, infected, or recovered at time t , respectively; the normalization condition implies that $S(t) + I(t) + R(t) = 1$. In Eq. 1, the term $\mu I(t)$ represents the recovery rate of the process $I \rightarrow R$ and the integral describes the infection process: i.e., $aS(t)P(s)$ is the activation rate of susceptible nodes into a cluster of size s and $[1 - (1 - \lambda I(s))^{s-1}]$ is the probability that such an activated susceptible node is infected by one of the remaining $s - 1$ individuals in the cluster; finally, we sum (integrate) over all the possible cluster sizes. The stability of the solution where all nodes are susceptible (i.e., $S = 1$, $I = 0$, and $R = 0$) can be studied by linearization. In particular, the linearization of the second of Eq. 1 gives

$$\partial_t I(t) = (-\mu + a\lambda \langle s(s-1) \rangle) I(t). \tag{2}$$

with $\langle s(s-1) \rangle = \int s(s-1)P(s)ds$ and the solution with $I = 0$, $R = 0$, and $S = 1$ is stable only if $\mu > a\lambda \langle s(s-1) \rangle$ and the basic reproduction number reads:

$$R_0 = \frac{a\lambda \langle s(s-1) \rangle}{\mu}. \tag{3}$$

The measure of the parameters in Eq. 3 is a difficult task. However, the expression for R_0 can be used to obtain a first estimate of the effect of a variation in the network connectivity on the epidemic propagation.

Since $s(s-1)/2$ is the number of links in a fully connected simplex of size s , Eq. 3 states that R_0 is proportional to the number of connections present in the system. As in the activity-driven models, individuals of a cluster are randomly reshuffled at each time step, correlation, and memory effect, characterizing the behavior of real temporal networks that are not included in this approach [40, 45].

Eq. 3 allows for a comparison among the three phases to estimate the change in the basic reproduction number due to the different size distribution $P(s)$ in the closing, partial opening, and total opening phases (Figure 4). In particular, R_0 increases from the closing to the partial opening phase as

$$\frac{R_{0,PO}}{R_{0,C}} = \frac{\langle s(s-1) \rangle_{PO}}{\langle s(s-1) \rangle_C} \approx 2.63 \tag{4}$$

while going from the partial opening to the total opening phase implies:

$$\frac{R_{0,TO}}{R_{0,PO}} = \frac{\langle s(s-1) \rangle_{TO}}{\langle s(s-1) \rangle_{PO}} \approx 13.03 \tag{5}$$

We verify that our estimates for the ratios in Eqs. 4, 5 are robust if we consider different time intervals to define the simplices from our data-set. In particular, for a time interval of 5 min, we obtain 2.91 and 12.36, while for a time interval of 30 min, we obtain 2.78 and 12.47 for the ratios in Eqs. 4 and 5, respectively.

We notice that the ratio between the total and partial opening phases is much larger than the ratio between the partial and closing phases. Therefore, while one could imagine controlling the spread with tracing measures in the transition from the closing to the partial opening period [10], the same kind of control would turn out to be ineffective in the transition to the total opening. However, we point out that in the total opening phase, a large percentage of the population had been vaccinated (about 80% in Italy), and the use of the Green Pass (mandatory for the access to the university buildings) implies that only vaccinated or tested people are admitted to the university buildings. Our data show that these additional measures are clearly necessary to limit the propagation in the total opening phase, due to the huge increase in the potentially dangerous contacts. Moreover, we notice that, in addition to tracing procedures, the use of masks and social distancing are still active even in the total opening period.

3.3 The link distribution at the access points

So far, we analyzed the sizes of groups that form in the university and we compared the distributions in the three phases with different restrictions. In particular, the data of simplex sizes can also be used to identify the most critical areas in the university, where large gatherings are more frequent. However, the formation of large groups is not the only relevant information to determine if an AP is critical. Indeed, if the large gatherings are due, e.g., to face-to-face lessons, we expect that the groups are stable for the whole duration of the lesson and that the contagion could be effectively traced (e.g., in the partially open period, an online seat reservation procedure was active). On the other hand, there could be places (such as an atrium) where small groups form, but they are continuously reshuffled. These places are typically dangerous because they host a high number of different contacts, many of which are very difficult to trace. For these reasons, we introduce a different characterization of the APs in order to find places where a large variety of contacts may occur. In particular, we define the *daily links* l_i of an AP as the number of contacts per day formed for more than 15 consecutive minutes between two different users in the same location. The index i hereafter labels the different APs. In this framework, if two users meet two or more times at the same point but at a different time, this is counted only once. Again, in the counting of user pairs, we have considered only the working time.

In order to test the effectiveness of the simplex size and of the daily link measure to characterize the critical locations, in Figure 6, we focus on two specific APs; one placed in a classroom of the teaching building and the other in the atrium of the physics department. In particular, panel c shows that in the partial opening period, the two APs have a similar size distribution $P_i(s)$ (simplices of size smaller than 5 cannot be reconstructed due to the anonymization procedure; see Supplementary Appendix). In this period, the average number of links $\langle s(s-1) \rangle_I = \int ds P_i(s) s(s-1)$ at the atrium is about 50% larger

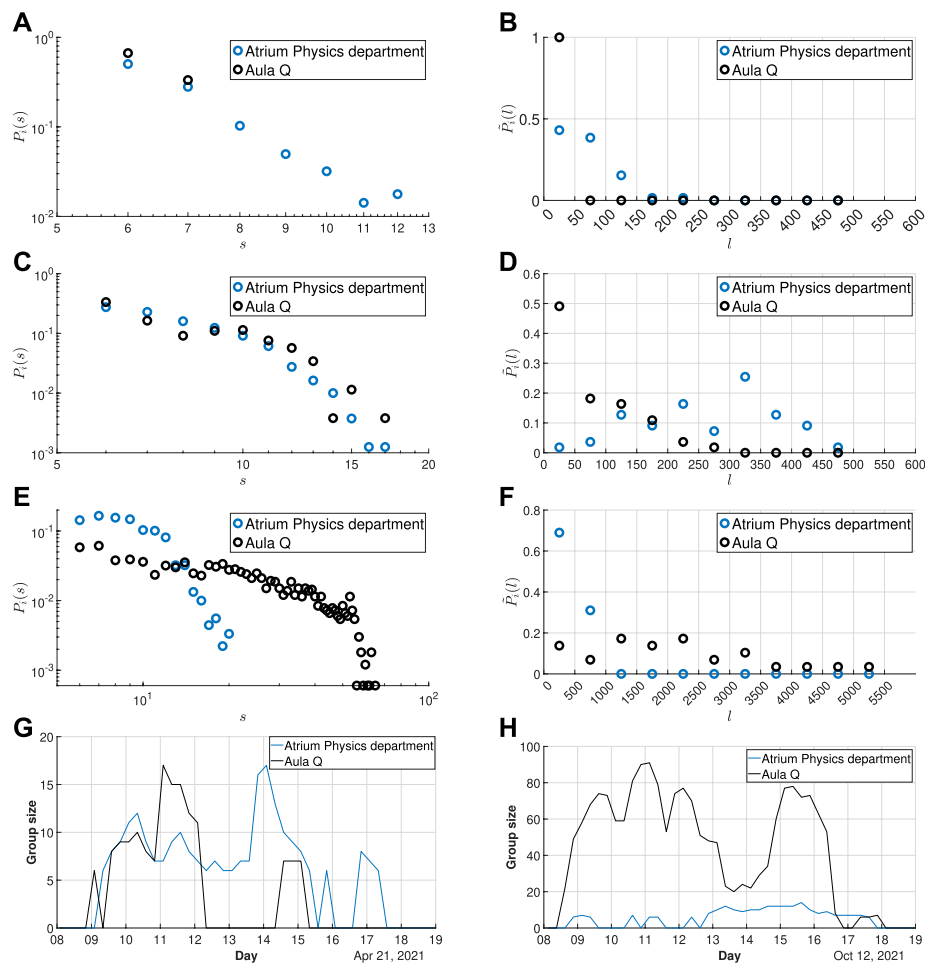


FIGURE 6

Comparison between different APs of the simplex size and daily link measures. We consider two APs installed in two different types of areas; one placed in a classroom and the other in the atrium of the physics department, and we compare their group size and daily link distributions. **(A,B)** Plot of group size distribution and daily link during the closing phase. The AP placed in the classroom shows that small groups are formed due to restrictions. **(C,D)** For the same APs, we plot the distributions obtained during the partial opening phase. The two APs have a similar group size distribution but different daily link distributions. This shows that the groups in the classroom are more stable than those in the atrium, where the groups are continuously reshuffled. **(E,F)** Plots show that large gatherings are formed in the classroom due to the return of face-to-face lessons. **(G,H)** Time evolution of the group size for the two APs during a typical working day in partial opening and total opening, respectively. For small groups with size $s < 6$, we have set the group size to 0.

than in the classroom ($\langle s(s-1) \rangle_i \approx 31.7$ v. s. $\langle s(s-1) \rangle_i \approx 19.0$). On the other hand, in the partial opening phase, the distribution of the number of different links per day $\bar{P}_i(l)$ turns out to be very different in the two APs. In particular, the average number of links per day is almost four times larger in the atrium than in the classroom ($\langle l \rangle_i \approx 270$ vs. $\langle l \rangle_i \approx 70$). This implies, as expected, a much more variable behavior of the contacts in the atrium. Panels **g** and **h** also show that in the atrium, the occupancy is almost constant during the working hours, while in the classroom, people assemble mainly during lessons. The data also show that people use the two areas differently in the periods we examined. In the atrium, the average link number increases from $\langle l \rangle_i \approx 73$ in the closure period to $\langle l \rangle_i \approx 270$, reaching $\langle l \rangle_i \approx 445$ in the total opening phase, while in the

classroom, we observe a much rapid growth starting from $\langle l \rangle_i \approx 0.7$ (almost no use in the closure period) to $\langle l \rangle_i \approx 70$, up to $\langle l \rangle_i \approx 2030$ in the total opening phase. The fact that different locations are used very differently in the distinct regimes of restrictions is well-confirmed in **Figure 7**, where we plot the distribution of the duration of the daily contacts between pairs of individuals in the different regimes of restrictions, in the atrium and in the considered classroom. All distributions display a typical exponential decay with a characteristic timescale, and, as expected, the contacts in the atrium are typically shorter than in the classroom. Moreover, as the restrictions are removed, the duration of the connection in the classroom increases, as one would expect due to the larger number of lessons; however, in the atrium, the contact time becomes shorter,

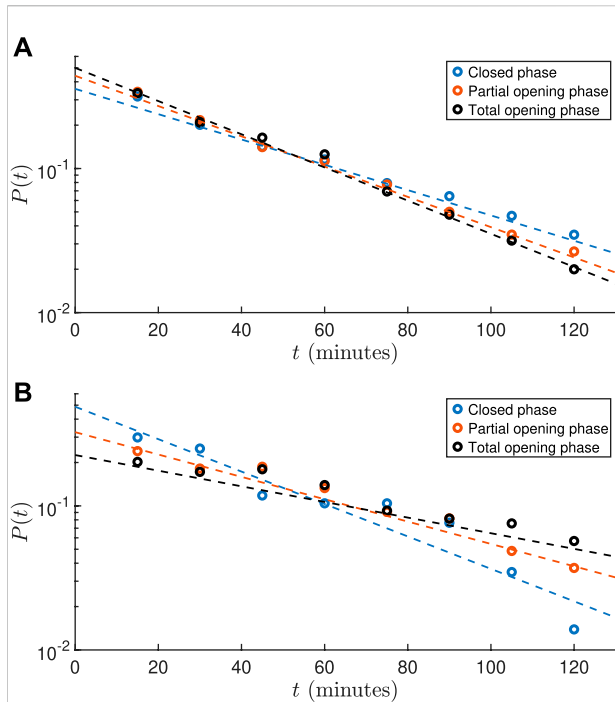


FIGURE 7
 Contact time distribution. Probability $P(t)$ that two users are in contact for a time t during working hours per day. **(A,B)** show the contact time distributions in the three different restriction regimes for the AP placed in the atrium of the physics department and classroom, respectively. We note that all distributions have an exponential decay $f(t) \propto e^{-t/\tau}$ but with different constant τ . For the contact time distributions related to the AP installed in the atrium of the physics department, we obtain a constant $\tau_C = 49 \pm 2$ m, $\tau_{PO} = 41 \pm 1$ m and $\tau_{TO} = 38 \pm 1$ m, while for the AP placed in the classroom, we obtain $\tau_C = 39 \pm 5$ m, $\tau_{PO} = 56 \pm 4$ m and $\tau_{TO} = 80 \pm 7$ m. We note that for the atrium of the physics department, the contact time decreases as the restrictions are removed, while in the classroom, the contact duration becomes longer in the opening periods.

showing a potential problem in monitoring the gatherings in common areas.

3.4 Optimal monitoring of spaces

The previous example shows that the distribution of the group sizes and that of the number of new links per day provide different information to identify critical areas. Therefore, to find the APs that need to be monitored first, in each phase, we characterize the AP i by the average number of different links per day $\langle I \rangle_i$ and also by the average number of links present in the relevant groups, that is, $\langle s(s-1) \rangle_i$. In Figures 10, 11, we show the APs with the largest $\langle I \rangle_i$ and $\langle s(s-1) \rangle_i$ in the partial and total opening period, respectively. There are cases of APs, particularly in study rooms and common areas, which gain more than fifteen positions in the ranking according to $\langle I \rangle_i$

compared to $\langle s(s-1) \rangle_i$, reaching the positions of critical APs. In this perspective, we notice that in the partial opening period, the atrium of the physics department considered in the previous section is ranked 16-th according to $\langle s(s-1) \rangle_i$ and 9-th according to $\langle I \rangle_i$, while the classroom moves from 24-th to 60-th position with the link ranking. This confirms that the two quantities classify the university areas differently according to their use. For potentially dangerous locations, the formation of large groups provides important information, but the relevant measure is the number of links between different users. A high number of daily links implies a continuous reshuffling of users who could trigger superspreading events. Therefore, the classification by average daily links of the APs appears to be the most relevant classification for determining the critical areas of the university campus.

Figures 10, 11 also show that the location of critical AP completely changes in the partial and total opening phases. This is due to the fact that some teaching activities with a large number of students, such as in engineering and in economics, were still held completely remotely in the partial opening period. For this reason, the relevant areas with typically substantial attendance remained almost empty in the partial opening period. This is shown in Figure 8 where on a city map we highlight with different colors the university buildings according to the number of APs present in Figure 10 or Figure 11, in the partial and total opening periods, respectively. In particular, we plot in light blue the buildings where there are no APs in the critical lists, in yellow the buildings where there are one or two critical APs, and in red the buildings where there are more than two critical APs in the lists.

Figure 9 shows how $\langle I \rangle_i$ and $\langle s(s-1) \rangle_i$ are distributed among the different APs. In order to plot the data on the same scale, both quantities are normalized by their average over the different APs (i.e., $\overline{\langle s(s-1) \rangle} = \frac{1}{N_{AP}} \sum_{i=1}^{N_{AP}} \langle s(s-1) \rangle_i$, $\overline{\langle I \rangle} = \frac{1}{N_{AP}} \sum_{i=1}^{N_{AP}} \langle I \rangle_i$, where N_{AP} is the total number of APs). We notice that the distributions feature slow decay at large values, which corresponds to the critical AP described in Figures 10, 11, i.e., the data above the vertical dashed lines in the figure.

3.5 Beyond the simplicial temporal network

The basic estimated reproduction number R_0 that we show in Section 3.2 has been evaluated on a temporal network model with simplices in a mean field approach without memory [9, 10]. This means that it is assumed that all the $s(s-1)/2$ links formed in the group of size s occur between nodes that are always different, with a total reshuffling at each time step. However, in our data, we observe that links between the same users usually repeat at the same location (i.e., AP) and probably also at different places, leading to an

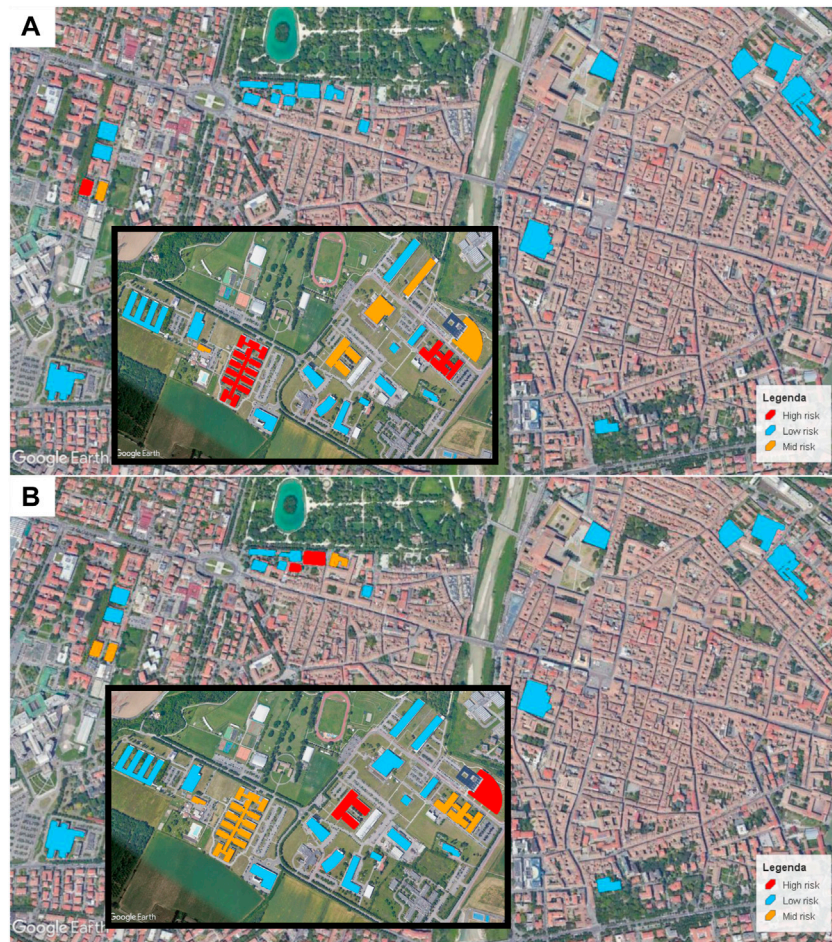


FIGURE 8
 Geographical map of buildings with critical APs. Map of Parma with the university buildings in three different colors based on the number of critical APs inside. **(A)** refers to the APs' rank in **Figure 10** of the partial opening period, while **(B)** refers to the total opening period with the ranking of the APs given in **Figure 11**. The light blue color represents the buildings where there are no APs in the critical list, the yellow buildings where there are one or two critical APs, and the red buildings where there are more than two critical APs in the list. The return of face-to-face lessons completely changes the location of critical APs to different buildings, such as in the economics department.

overestimate of the number of contacts. Moreover, we have shown that link repetition displays different timescales in the different restriction regimes and in the different locations. From this perspective, contact reshuffling may have a significant effect on epidemic spread even in the comparison among the different phases of restrictions.

In the previous section, we outlined the measured AP link distribution. This quantity gives the number of different pairs per day formed for more than 15 min at each AP. In order to estimate the global effect of the contact reshuffling in the different phases, we can also consider how many different couples \mathcal{L}_d are formed every day in the whole university and compare the behavior of this quantity in the different regimes. This integrated global data have been directly calculated by the “ICT services” office as discussed in [Supplementary](#)

Appendix. The ratio between the average number of different pairs per day in the partial opening and in the closing phase is

$$\frac{\langle \mathcal{L}_d \rangle_{PO}}{\langle \mathcal{L}_d \rangle_C} \approx 3.70 \tag{6}$$

We notice that the ratio obtained considering different links (**Eq. 6**) is significantly larger than the ratio obtained considering the total number of links given in (**Eq. 4**). This means that in the passage from partial opening to a closing period, not only the size of the groups is significantly reduced but also the variability of contacts is even more suppressed. This could be due to the different behaviors of students and university staff. In particular, as already observed, in the closing phase, the presence of students is reduced, and this probably strongly limits the flows between

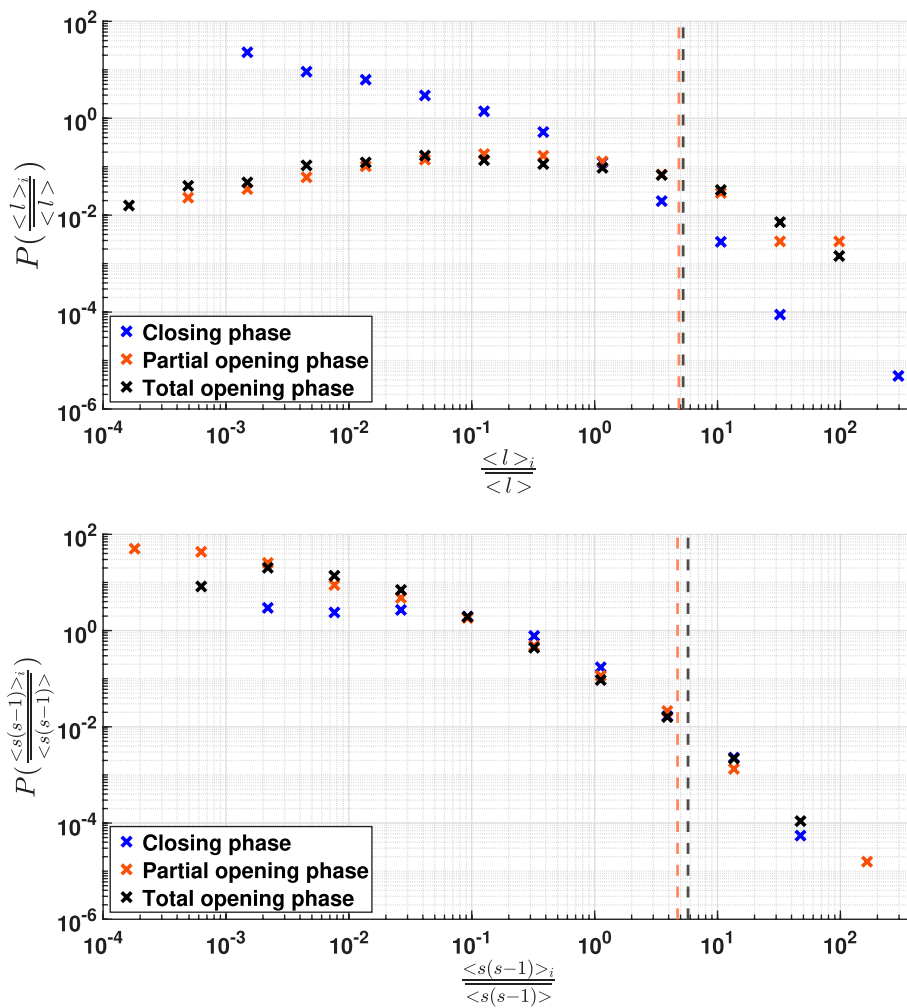


FIGURE 9 Link distribution among the different APs. The plots show how the average number of different links per day $\langle l \rangle_i$ and average links $\langle s(s-1) \rangle_i$ are distributed among the different APs. Both quantities are normalized by their average over the different APs. The dashed lines correspond to the thresholds that give the critical APs in Figures 10, 11. There is a different distribution for the closing period compared to the opening phases, clarifying that groups are more stable in the closing phase.

the different departments, due to face-to-face lessons, and the use of common areas. On the other hand, staff members, in particular in the closing period, tend to establish contacts only with people within their own laboratory, displaying, therefore, a more stable pattern of contacts.

Finally, we measure the ratio of the average number of different links per day in the total and in the partial opening phase:

$$\frac{\langle \mathcal{L}_d \rangle_{TO}}{\langle \mathcal{L}_d \rangle_{PO}} \approx 12.98 \tag{7}$$

In this case, the ratio we obtain is very similar to the ratio observed between $\langle s(s-1) \rangle$ in the same phases. This seems to suggest that the effect of link reshuffling vs. link repetition is

stable in the transition between these two phases, and only a global rescaling of the total number of contacts is observed. We notice that now in both periods, the presence of students and lessons is dominant. Therefore, the same type of space fruition takes place in the two phases in the university, while, as we observed above, in the closing regime, the laboratory activity provides a more stable pattern of link formation.

Our estimates for the ratio of the average number of different pairs and the average number of different links per day in the two periods are robust if we change the time intervals used to define simplices. In particular, if the formation of the simplex is defined using a time interval of 5 min, we obtain the values 3.56 and 12.50 for the ratios in Eqs

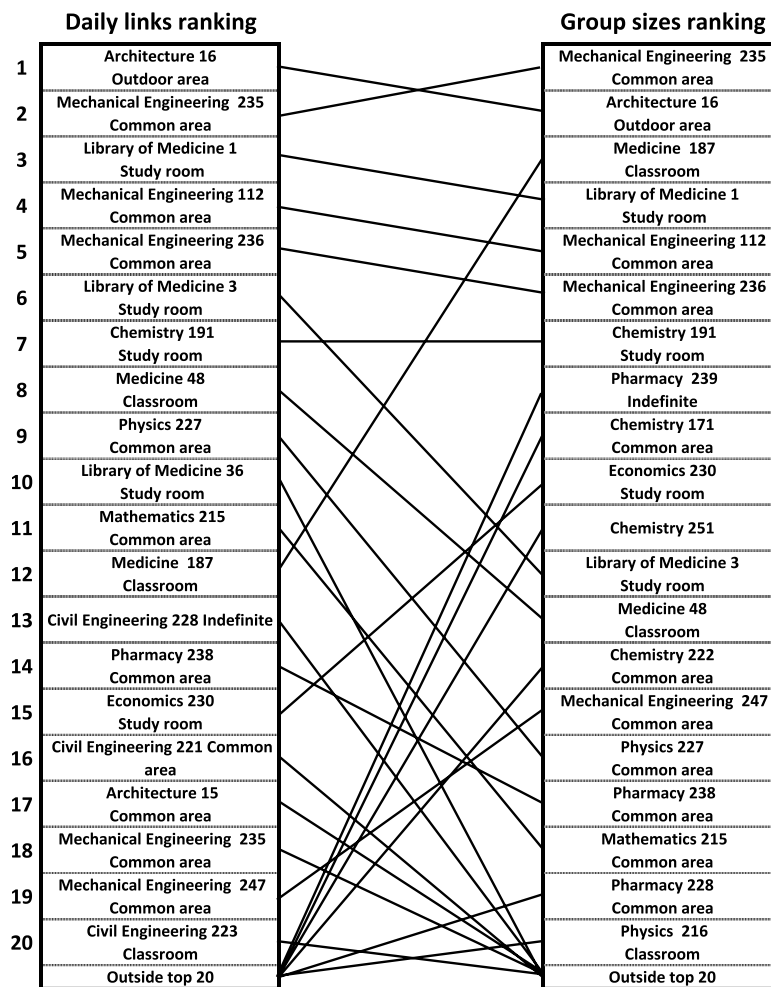


FIGURE 10
Rankings during the partial opening phase. The top twenty positions in the ranking by link distributions during the partial opening phase compared with positions in the ranking by the size of groups.

6, 7, respectively, while for a time interval of 30 min, the results are 3.64 and 13.33.

The different behavior characterizing the closing period with respect to the partial and total opening phases is also shown in Figure 9. The distribution among the different APs is very similar in the two opening phases, and they differ only for a global rescaling. This confirms that in the opening phases, different areas are occupied in a similar way, with an analogous reshuffling mechanism and only a global shift in the number of presences. Interestingly, such regular behavior characterized by a global rescaling occurs even if the location of the critical APs drastically changes in the two periods, as evidenced by Figure 8. On the other hand, in the closing period, the distributions in Figure 9 are significantly different even after the global rescaling. In particular, the distribution of $\langle I \rangle_i$ shows a sharper behavior, indicating that areas characterized by a reshuffling significantly

larger than the average are very rare in the period without didactic activity.

4 Discussion

Data from Wi-Fi networks provide an efficient way to monitor in (almost) real time space occupancy and mobility of users in restricted areas. These data can represent an interesting resource for maintaining continuous monitoring in public spaces during the period of control of the epidemic that surely awaits us in the coming years. Here, we used anonymized data to signal the most used areas of a university campus in three different periods with distinct containment measures. We classify the university areas according to two different quantities: the typical size of groups and the average number of links between different users formed in

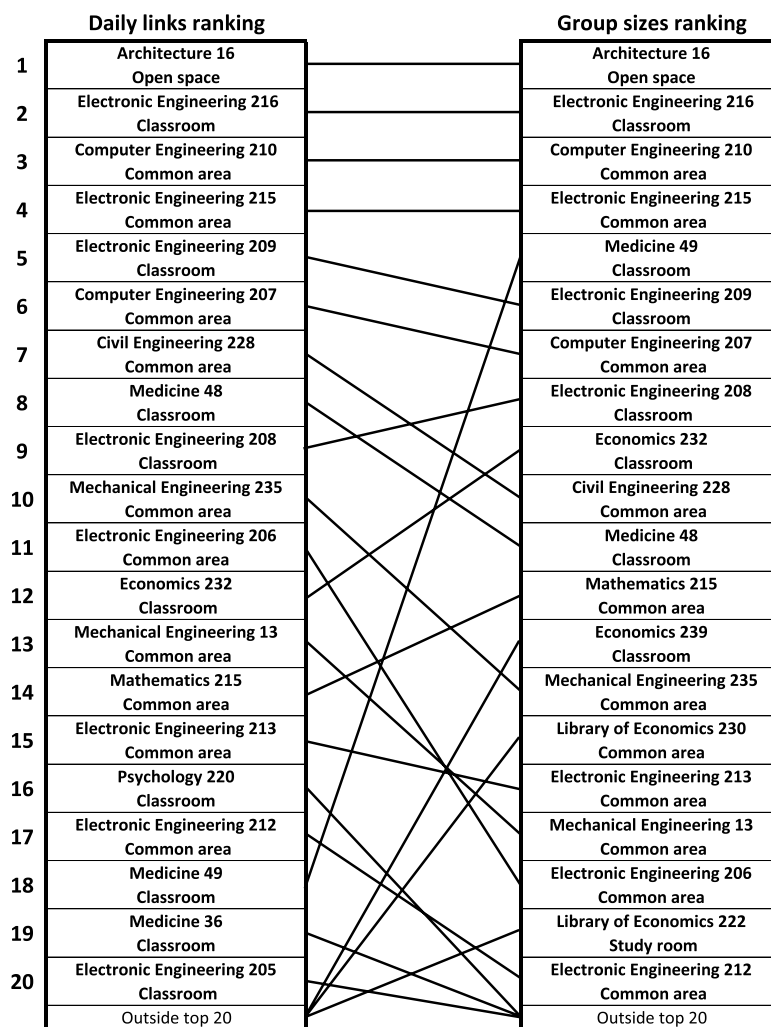


FIGURE 11
Rankings during the total opening phase. The top twenty positions in the ranking by link distributions during the total opening phase compared with positions in the ranking by the size of groups.

the area covered by the APs. Both of these quantities can be used to signal areas that are potentially dangerous due to the risk of the contagion, with the second one being related to areas of intense and uncontrolled traffic that are difficult to trace and riskier. Also, these quantities can be used to efficiently monitor the different fruition of spaces from distinct classes of users, such as staff and students. Within an approach to epidemic spreading on simplicial temporal networks, using the measured simplex size distribution as an input to the theory, our analysis also provides a specific estimate of the dramatic change in the reproduction number occurring in the total opening phase due to the increasing of contacts [10].

Notably, Wi-Fi data, further anonymized also with respect to locations, can provide a useful source to build an experimental temporal network to test specific epidemic models [34]. In

particular, it would be very interesting to compare the results obtained from epidemic spreading on the real network to the mean field formulation to test the efficacy of mean field approximations.

Beyond applications to epidemic models, Wi-Fi data represent a natural tool to obtain the structure and the evolution of groups of people that move and connect in the same spatial environment. In particular, Wi-Fi measurements allow us quite naturally to detect the presence of more complex nested sub-structures (motifs) other than fully connected simplices, as evidenced in several contexts [46]. For these reasons, Wi-Fi data may be of potential interest for applications of higher-order interaction models in different fields, such as opinion dynamics, social cooperation, and complex contagion [11–13].

A further extension of our work is the analysis of other public and private spaces with a focus on public transportation, including Wi-Fi on buses. In this context, it will also be very

interesting to analyze the impact of multi-modal monitoring solutions, for example, combining Wi-Fi, cellular, and video-based localization. We foresee that such multi-modal technologies could compensate for each other's limitations, enabling us to analyze wide areas, while limiting privacy impact.

The use of such fine-grained passive monitoring technologies could be very useful for conducting natural experiments to evaluate the impact of policies and mechanisms to steer people's behaviors. For example, we plan to use this approach to evaluate the impact of COVID-related notices and signage on people crowding.

Data availability statement

The raw data supporting the conclusions of this article will be made available by the authors without undue reservation.

Author contributions

RB, AG, MM, and AV designed the research; AG analyzed data; AG, AB, and CV and FR collected data; RB, AG, MM, and AV wrote the manuscript. All authors read and approved the final manuscript.

Funding

RB, AG, and AV acknowledge support from the EU-PON Project POR FSE Emilia Romagna 2018/2020 Objective 10.

References

- Gast MS. *802.11 wireless networks: The definitive guide (O'reilly)* (2005).
- Redondi AE, Cesana M, Weibel DM, Fitzgerald E. Understanding the wifi usage of University students. In: *2016 international wireless Communications and mobile computing conference*. Sebastopol, USA: IWCMC (2016). p. 44–9. doi:10.1109/IWCMC.2016.7577031
- Sapiezynski P, Stopczynski A, Gatej R, Lehmann S. Tracking human mobility using wifi signals. *PLOS ONE* (2015) 10:e0130824–11. doi:10.1371/journal.pone.0130824
- Luo C, Cheng L, Chan MC, Gu Y, Li J, Ming Z, Pallas: Self-bootstrapping fine-grained passive indoor localization using wifi monitors. *IEEE Trans Mob Comput* (2017) 16:466–81. doi:10.1109/TMC.2016.2550452
- Lau MSY, Grenfell B, Thomas M, Bryan M, Nelson K, Lopman B. Characterizing superspreading events and age-specific infectiousness of sars-cov-2 transmission in Georgia, USA. *Proc Natl Acad Sci U S A* (2020) 117:22430–5. doi:10.1073/pnas.2011802117
- Cattuto C, Van den Broeck W, Barrat A, Colizza V, Pinton JF, Vespignani A. Dynamics of person-to-person interactions from distributed rfid sensor networks. *PLOS ONE* (2010) 5:e11596. doi:10.1371/journal.pone.0011596
- Isella L, Stehlé J, Barrat A, Cattuto C, Pinton JF, Van den Broeck W. What's in a crowd? Analysis of face-to-face behavioral networks. *J Theor Biol* (2011) 271:166–80. doi:10.1016/j.jtbi.2010.11.033
- Machens A, Gesualdo F, Rizzo C, Tozzi AE, Barrat A, Cattuto C. An infectious disease model on empirical networks of human contact: Bridging the gap between dynamic network data and contact matrices. *BMC Infect Dis* (2013) 13:185. doi:10.1186/1471-2334-13-185
- Petri G, Barrat A. Simplicial activity driven model. *Phys Rev Lett* (2018) 121:228301. doi:10.1103/PhysRevLett.121.228301
- Mancastroppa M, Guizzo A, Castellano C, Vezzani A, Burioni R. Sideward contact tracing and the control of epidemics in large gatherings. *J R Soc Interf* (2022) 19:20220048. doi:10.1098/rsif.2022.0048
- Iacopini I, Petri G, Barrat A, Latora V. Simplicial models of social contagion. *Nat Commun* (2019) 10:2485. doi:10.1038/s41467-019-10431-6
- Battiston F, Cencetti G, Iacopini I, Latora V, Lucas M, Patania A, et al. Networks beyond pairwise interactions: Structure and dynamics. *Phys Rep networks Beyond Pairwise Interactions: Struct Dyn* (2020) 874:1–92. doi:10.1016/j.physrep.2020.05.004
- Battiston F, Amico E, Barrat A, Bianconi G, Guilherme FA, Franceschiello B, et al. Networks beyond pairwise interactions: Structure and dynamics. *Nat Phys* (2021) 17:1093–8. The physics of higher-order interactions in complex systems. doi:10.1038/s41567-021-01371-4
- Mancastroppa M, Burioni R, Colizza V, Vezzani A. Active and inactive quarantine in epidemic spreading on adaptive activity-driven networks. *Phys Rev E* (2020) 102:020301. doi:10.1103/PhysRevE.102.020301
- Mancastroppa M, Castellano C, Vezzani A, Burioni R. Stochastic sampling effects favor manual over digital contact tracing. *Nat Commun* (2021) 12:1919. doi:10.1038/s41467-021-22082-7
- Sapiezynski P, Stopczynski A, Wind DK, Leskovec J, Lehmann S. Inferring person-to-person proximity using wifi signals. *Proc ACM Interact Mob Wearable Ubiquitous Technol* (2017) 1:1–20. doi:10.1145/3090089

Acknowledgments

We warmly thank Marco Mancastroppa and Andrea Prati for their very useful comments and suggestions.

Conflict of interest

The authors declare that the research was conducted in the absence of any commercial or financial relationships that could be construed as a potential conflict of interest.

Publisher's note

All claims expressed in this article are solely those of the authors and do not necessarily represent those of their affiliated organizations, or those of the publisher, the editors, and the reviewers. Any product that may be evaluated in this article, or claim that may be made by its manufacturer, is not guaranteed or endorsed by the publisher.

Supplementary material

The Supplementary Material for this article can be found online at: <https://www.frontiersin.org/articles/10.3389/fphy.2022.1010929/full#supplementary-material>

17. Zhou M, Ma M, Zhang Y, Sui A K, Pei D, Moscibroda T. Edum: Classroom education measurements via large-scale wifi networks. In: *Proceedings of the 2016 ACM international joint conference on pervasive and ubiquitous computing*. New York, NY, USA: Association for Computing Machinery (2016). p. 316–27. UbiComp '16.
18. Kim M, Kotz D, Kim S. Extracting a mobility model from real user traces. In: *Proceedings IEEE INFOCOM 2006. 25TH IEEE international conference on computer Communications* (2006). p. 1–13.
19. Chen G, Kotz D. *A case study of four location traces* (2004). Available at: https://digitalcommons.dartmouth.edu/cs_tr/246/.
20. Cisco Unified Wireless Location-Based Services. *Cisco Unified Wireless Location-Based Services* (2021). Available at: <https://www.cisco.com/en/US/docs/solutions/Enterprise/Mobility/emob30dg/Locatn.html> (Accessed 11 29, 2021).
21. Han K, Yu SM, Kim SL, Ko SW. Exploiting user mobility for wifi rtt positioning: A geometric approach. *IEEE Internet Things J* (2021) 8:14589–606. doi:10.1109/JIOT.2021.3070367
22. Sharma A, Li J, Mishra D, Batista G, Seneviratne A. Passive wifi csi sensing based machine learning framework for covid-safe occupancy monitoring. In: *2021 IEEE international conference on Communications workshops (ICC workshops)* (2021). p. 1–6. doi:10.1109/ICCWorkshops50388.2021.9473673
23. Huang B, Mao G, Qin Y, Wei Y. Pedestrian flow estimation through passive wifi sensing. *IEEE Trans Mob Comput* (2021) 20:1529–42. doi:10.1109/TMC.2019.2959610
24. Ahmed N, Michelin RA, Xue W, Rui S, Malaney R, Kanhere SS, et al. A survey of Covid-19 contact tracing apps. *IEEE Access* (2020) 8:134577–601. doi:10.1109/ACCESS.2020.3010226
25. Jiang T, Zhang Y, Zhang M, Yu T, Chen Y, Lu C, et al. A survey on contact tracing: The latest advancements and challenges. *ACM Trans Spat Algorithms Syst* (2022) 8:1–35. doi:10.1145/3494529
26. Eagle N, Sandy Pentland A. Reality mining: Sensing complex social systems. *Pers Ubiquitous Comput* (2006) 10:255–68. doi:10.1007/s00779-005-0046-3
27. Oliver N, Lepri B, Sterly H, Lambiotte R, Deletaille S, Nadai MD, et al. Mobile phone data for informing public health actions across the Covid-19 pandemic life cycle. *Sci Adv* (2020) 6:eabc0764. doi:10.1126/sciadv.abc0764
28. Cristani M, Bue AD, Murino V, Setti F, Vinciarelli A. The visual social distancing problem. *IEEE Access* (2020) 8:126876–86. doi:10.1109/ACCESS.2020.3008370
29. Mokbel MF, Xiong L, Zeinalipour-Yazdi D. Introduction to the special issue on contact tracing. *ACM Trans Spat Algorithms Syst* (2022) 8:1–2. doi:10.1145/3514137
30. Zakaria C, Trivedi A, Chee M, Shenoy PJ, Balan R. *Analyzing the impact of covid-19 control policies on campus occupancy and mobility via passive wifi sensing* (2020). CoRR abs/2005.12050.
31. Mu M. *Wifi-based crowd monitoring and workspace planning for COVID-19 recovery* (2020). CoRR abs/2007.12250.
32. Cecchet E, Acharya A, Molom-Ochir T, Trivedi A, Wifimon SP. A mobility analytics platform for building occupancy monitoring and contact tracing using wifi sensing: Poster abstract. In: *Proceedings of the 18th conference on embedded networked sensor systems*. New York, NY, USA: Association for Computing Machinery (2020). p. 792–3. SenSys '20. doi:10.1145/3384419.3430598
33. Gupta P, Mehrotra S, Panwar N, Sharma S, Venkatasubramanian N, Wang G. *Quest: Practical and oblivious mitigation strategies for COVID-19 using wifi datasets* (2020). CoRR abs/2005.02510.
34. Das Swain V, Xie J, Madan M, Sargolzaei S, Cai J, De Choudhury M, et al. *Wifi mobility models for covid-19 enable less burdensome and more localized interventions for university campuses* (2021). medRxiv. doi:10.1101/2021.03.16.21253662
35. Zakaria C, Trivedi A, Cecchet E, Chee M, Shenoy P, Balan R. Analyzing the impact of Covid-19 control policies on campus occupancy and mobility via wifi sensing. *ACM Trans Spat Algorithms Syst* (2022) 8:1–26. doi:10.1145/3516524
36. Stehlé J, Barrat A, Bianconi G. Dynamical and bursty interactions in social networks. *Phys Rev E* (2010) 81:035101. doi:10.1103/PhysRevE.81.035101
37. Zhao K, Stehlé J, Bianconi G, Barrat A. Social network dynamics of face-to-face interactions. *Phys Rev E* (2011) 83:056109. doi:10.1103/PhysRevE.83.056109
38. European Center for Disease Prevention and Control. *Resource estimation for contact tracing, quarantine and monitoring activities for covid-19 cases in the eu/eea*. Stockholm: European Centre for Disease Prevention and Control (2020). Available at: <https://www.ecdc.europa.eu/sites/default/files/documents/COVID-19-resources-for-contact-tracing-2-March-2020.pdf>.
39. Perra N, Gonçalves B, Pastor-Satorras R, Vespignani A. Activity driven modeling of time varying networks. *Sci Rep* (2012) 2:469. doi:10.1038/srep00469
40. Tizzani M, Lenti S, Ubaldi E, Vezzani A, Castellano C, Burioni R. Epidemic spreading and aging in temporal networks with memory. *Phys Rev E* (2018) 98:062315. doi:10.1103/PhysRevE.98.062315
41. Mancastroppa M, Vezzani A, Muñoz MA, Burioni R. Burstiness in activity-driven networks and the epidemic threshold. *J Stat Mech* (2019) 2019:053502. doi:10.1088/1742-5468/ab16c4
42. Johansson MA, Quandelacy TM, Kada S, Prasad PV, Steele M, Brooks JT, et al. SARS-CoV-2 transmission from people without COVID-19 symptoms. *JAMA Netw Open* (2021) 4:e2035057. doi:10.1001/jamanetworkopen.2020.35057
43. Guan WJ, Ni ZY, Hu Y, Liang WH, Ou CQ, He JX, et al. Clinical characteristics of coronavirus disease 2019 in China. *N Engl J Med Overseas Ed* (2020) 382:1708–20. doi:10.1056/NEJMoa2002032
44. World Health Organization. *Report of the WHO-China joint mission on coronavirus disease 2019* (2020). (COVID-19). Available at: <https://www.who.int/docs/default-source/coronaviruse/who-china-joint-mission-on-covid-19-final-report.pdf>.
45. Ubaldi E, Perra N, Karsai M, Vezzani A, Burioni R, Vespignani A. Asymptotic theory of time-varying social networks with heterogeneous activity and tie allocation. *Sci Rep* (2016) 6:35724. doi:10.1038/srep35724
46. Lotito QF, Musciotto F, Montresor A, Battiston F. Higher-order motif analysis in hypergraphs. *Commun Phys* (2022) 5:79. doi:10.1038/s42005-022-00858-7
47. Finck M, Pallas F. They who must not be identified—Distinguishing personal from non-personal data under the GDPR. *Int Data Privacy L* (2020) 10:11–36. doi:10.1093/idpl/ipz026
48. Council of the European Union. *Regulation on privacy and electronic Communications* (2018). Available at: <https://data.consilium.europa.eu/doc/document/ST-5008-2021-INIT/en/pdf>.